



# Development of a galvanic sensor system for detecting the corrosion damage of the steel embedded in concrete structures: Part 1. Laboratory tests to correlate galvanic current with actual damage

Ji-Hong Yoo<sup>a</sup>, Zin-Taek Park<sup>a</sup>, Jung-Gu Kim<sup>a,\*</sup>, Lan Chung<sup>b</sup>

<sup>a</sup>Department of Advanced Materials Engineering, Sung Kyun Kwan University, 300 Chunchun-Dong, Jangan-Gu, Suwon, 440-746, Republic of Korea

<sup>b</sup>Department of Architectural Engineering, Dankook University, Hannam-Dong, Yongsan-Gu, Seoul, 140-210, Republic of Korea

Received 17 December 2002; accepted 2 July 2003

## Abstract

The correlation between sensor output and corrosion rate of reinforcing steel was evaluated by laboratory electrochemical tests in saturated  $\text{Ca}(\text{OH})_2$  with 3.5 wt.% NaCl. In this paper, two types of electrochemical probes were developed: galvanic cells containing of steel/copper and steel/stainless steel couples. The corrosion behavior in saturated  $\text{Ca}(\text{OH})_2$  solution with and without 3.5 wt.% NaCl addition for the different electrodes was investigated by potentiodynamic test. Weight loss measurement and galvanic corrosion test were conducted to obtain the corrosion rate of reinforcing steel and the charge of sensor in saturated  $\text{Ca}(\text{OH})_2$  solution with 3.5 wt.% NaCl addition, respectively.

The results of the potentiodynamic test indicated the possibility of detecting an ingress point of chlorides by measuring the galvanic current. In galvanic corrosion tests, the galvanic current of steel/copper couple was higher than that of steel/stainless steel couple, i.e., the steel/copper sensor is more suitable for high resistance environment. The steel/stainless sensor showed a better linear correlation than the steel/copper sensor. Through the relationship between the sensor system output and the weight loss ( $\text{mg}/\text{cm}^2$ ) of steel, real corrosion damage of the steel embedded in concrete can be detected.

© 2003 Elsevier Ltd. All rights reserved.

**Keywords:** Galvanic sensor system; Concrete; Corrosion; Pore solution; Chloride

## 1. Introduction

Reinforced concrete is a versatile, economical and successful construction material. It is durable and strong, performing well throughout its service life. However, the corrosion of reinforcing steel in concrete is becoming an issue in the collapse of the concrete structures as engineers and surveyors maintain an aging infrastructure in recent years. Usually, the steel embedded in concrete becomes passivated due to the initial high alkalinity ( $12 < \text{pH} < 13$ ) of the pore solution. However, the protective film is destroyed and the reinforcing steel is depassivated when sufficient chloride ions (from deicing salts or from seawater) have penetrated to the reinforcement or when the pH of the pore

solution drops to low values due to carbonation. Corrosion in the form of rust formation and/or loss in cross section of the reinforcing steel occurs in the presence of oxygen and water. The corrosion of steel in concrete essentially is an electrochemical process, where at the anode, iron is oxidized to iron ions that pass into solution and at the cathode, oxygen is reduced to hydroxyl ions. Anode and cathode form a short-circuited corrosion cell, with the flow of electrons in the steel and of ions in the pore solution of the concrete. The corrosion between actively corroding areas of the reinforcing steel and passive areas is of great concern because it results in very high local anodic current densities with corrosion rates of 0.5–1 mm/year. The resulting local loss in cross section has dangerous implications for the structural safety if the corroded steels are located in a zone of high tensile or shear stresses [1–6].

Many new systems and materials have been developed to delay the onset of corrosion and to increase durability. However, there is only limited success in delaying the time

\* Corresponding author. Tel.: +82-31-290-7360; fax: +82-31-290-7371.

E-mail address: [kimjg@skku.ac.kr](mailto:kimjg@skku.ac.kr) (J.-G. Kim).

to corrosion. In view of economic and engineering points, quantitative assessment of corrosion is also important. Thereby, sensor systems are needed to enable owners of the structures to monitor the corrosion risk and to take protective measures before the damaging processes start. It must be more economical to remove and replace the areas of active reinforcement corrosion only rather than to remove all the chloride-contaminated concrete, particularly in areas where active reinforcement corrosion had not started [7]. However, techniques for inspection and monitoring of the corrosion of reinforcing steel in concrete structures are at present limited to either mechanical inspection, chemical analysis or isopotential (half-cell) mapping. In all cases, these techniques cannot supply information on the corrosion rate occurring but only provide information of the presence of corrosion.

The purpose of this research is to develop corrosion monitoring sensor system, which can detect corrosion problems on a reinforced concrete structure quantitatively. It uses well-known principles of galvanic corrosion and consists of two dissimilar metals, which provide current because of a natural voltage difference.

## 2. Experimental details

### 2.1. Preparation for materials and solution

The anode material used in the present investigation was Korean standards (KS) D 3504 (steel bars for concrete reinforcement) with the chemical composition of 0.22 C, 0.14 Si, 0.59 Mn, 0.02 P, 0.025 S and balanced Fe (in wt.%). Type 304 austenitic stainless steel (UNS S30400) and pure copper were used as the cathode materials. All specimens were machined in the shape of a bar with a diameter of 12 mm and polished with a 600 silicon carbide (SiC) grit emery paper. After grinding, the samples were ultrasonically cleaned, rinsed with ethanol and dried.

The electrochemical behavior of the specimens was examined under two conditions. First, the electrodes were immersed directly in saturated  $\text{Ca(OH)}_2$  solution to reproduce the pore solution of concrete normally, and secondly, the electrodes were immersed in saturated  $\text{Ca(OH)}_2$  solution with 3.5 wt.% NaCl addition to represent environments of sufficient chloride ions (from deicing salts or from seawater) penetrated to the reinforcement.

### 2.2. Potentiodynamic polarization test

The potentiodynamic polarization tests were performed to evaluate the overall corrosion behavior of the anode and cathode materials. Measurements of electrochemical polarization were conducted using an EG & G 273A potentiostat. The electrochemical polarization cell consisted of graphite counter electrode, saturated calomel electrode (SCE) and a working electrode (WE).

The potential of the sample was swept at a rate of 600 mV/h from the initial potential of  $-0.25$  V versus open-circuit potential (OCP) to the final potential of  $+1.5$  V versus SCE. The experiments were started when the corrosion potential did not changed by more than 1 mV/min within 20 min. The potentiodynamic tests were conducted at ambient laboratory temperature. The potentiodynamic data were used in Tafel extrapolation to calculate corrosion rates. All potentials are reported with respect to SCE. To insure reproducibility, at least three measurements were run for each specimen.

### 2.3. Immersion test

Immersion tests were conducted in saturated  $\text{Ca(OH)}_2$  solution with 3.5 wt.% NaCl addition with the anode materials at ambient temperature, and specimens were taken out from solution periodically. A concentrated hydrochloric acid solution was used to clean the corrosion products off the steel as described in ASTM G 1. Then, specimens were dried in an oven at  $80^\circ\text{C}$  for 1 h and weighed to 0.1 mg.

After the immersion test was completed, corrosion products on the metal surface were investigated by means of scanning electron microscopy (SEM) and X-ray photoelectron spectroscopy (XPS).

### 2.4. Galvanic corrosion test

Galvanic corrosion tests were accomplished in saturated  $\text{Ca(OH)}_2$  solution with 3.5 wt.% NaCl addition with steel/copper and steel/stainless steel (Type 304) at ambient temperature. Galvanic current measurements were made with a zero-resistance ammeter. Fig. 1 shows the experimental arrangement. One electrode was connected to the WE terminal, the other to the reference electrode (REF)

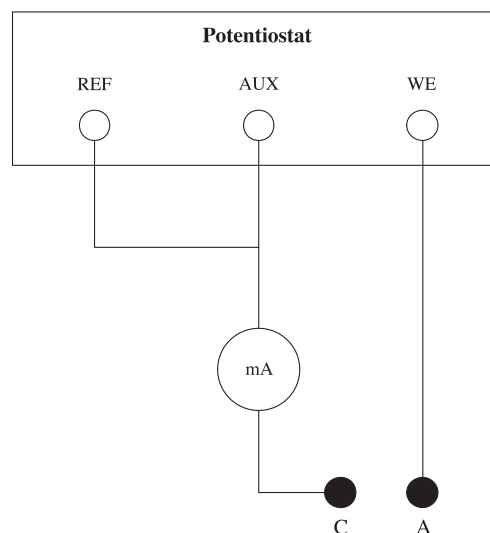


Fig. 1. Zero resistance ammeter for measurement of galvanic current at shot circuit.

terminal, which was connected to the auxiliary (AUX) electrode.

### 3. Results and discussion

#### 3.1. Potentiodynamic polarization test

Fig. 2 shows the open-circuit potentials and the potentiodynamic polarization curves of steel, stainless steel and copper in saturated  $\text{Ca}(\text{OH})_2$  solution. The potentials of specimens tend to increase during the immersion time. Particularly, the potentials of steel increased rapidly in the initial stage of immersion from  $-330$  mV (SCE) to  $-130$  mV (SCE). In chloride-free solution, all specimens are passivated due to the high alkalinity ( $12 < \text{pH} < 13$ ) of the pore solution. If steel is coupled to the cathode materials under such conditions, the galvanic current between the anode material and the cathode material will be negligibly low due to the small difference between open-circuit potentials [8].

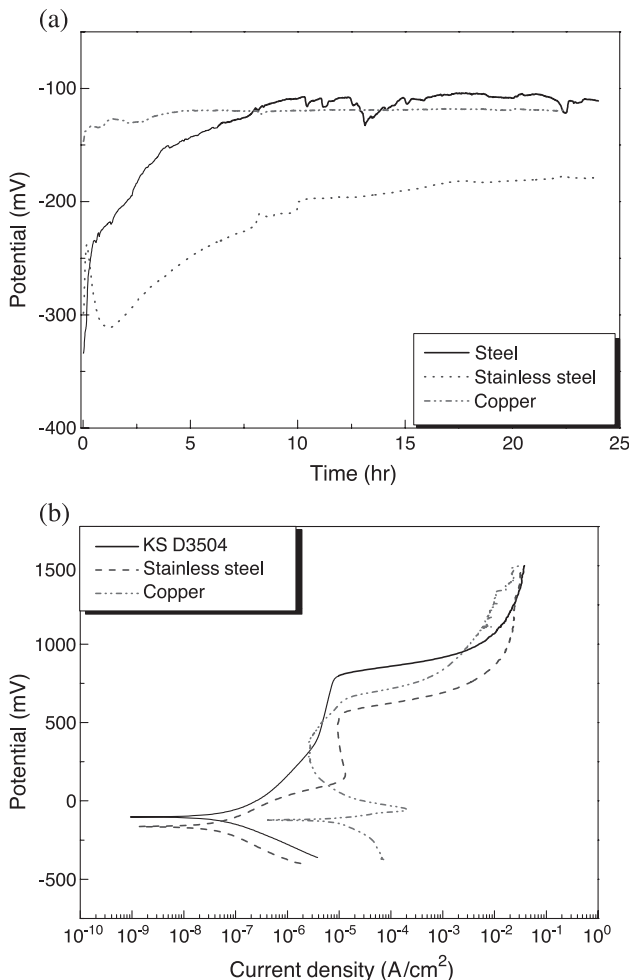


Fig. 2. Open-circuit potentials and anodic polarization curves of specimens in saturated  $\text{Ca}(\text{OH})_2$  solution.

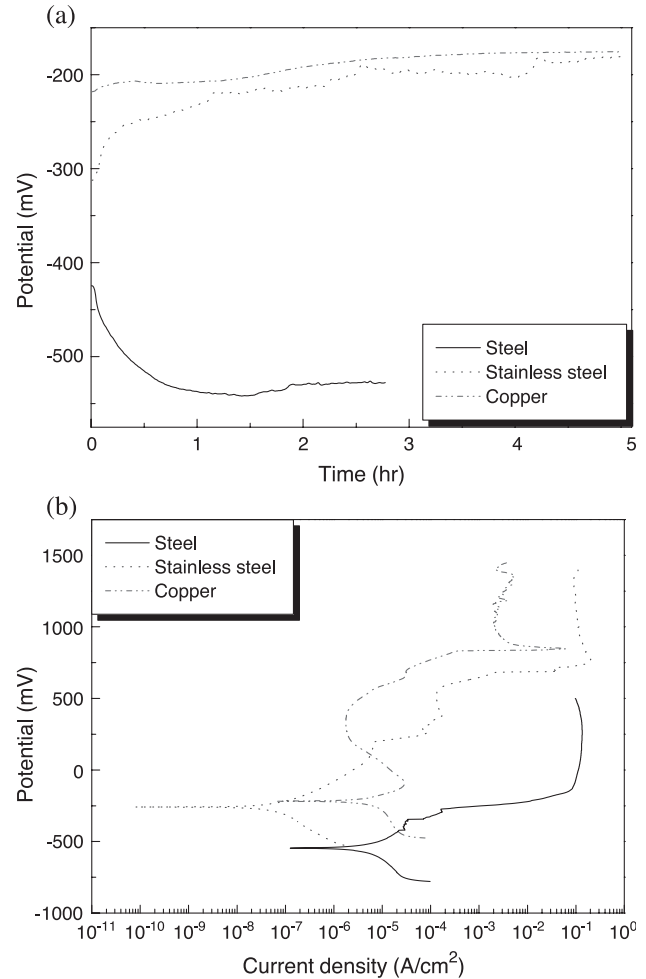


Fig. 3. Open-circuit potentials and anodic polarization curves of specimens in saturated  $\text{Ca}(\text{OH})_2$  with 3.5 wt.% NaCl solution.

Fig. 3 shows the open-circuit potentials and the potentiodynamic polarization curves of steel, stainless steel and copper in saturated  $\text{Ca}(\text{OH})_2$  solution with 3.5 wt.% NaCl addition. The potentials of stainless steel and copper increased slightly and stabilized with the immersion time. However, the potential of steel decreased rapidly in the initial stage of immersion. The reason for this is that chloride ions destroyed the passive films of

Table 1

Result of corrosion potential and corrosion rate measurements in different solutions

Solution		KS D 3504	Stainless steel	Copper
Saturated $\text{Ca}(\text{OH})_2$	$E_{\text{corr}}$ (mV)	-102	-164	-127
	Corrosion rate (mpy)	0.03	0.01	3.75
Saturated $\text{Ca}(\text{OH})_2$ with 3.5 wt.% NaCl addition	$E_{\text{corr}}$ (mV)	-546	-225	-220
	Corrosion rate (mpy)	1.90	0.04	3.82

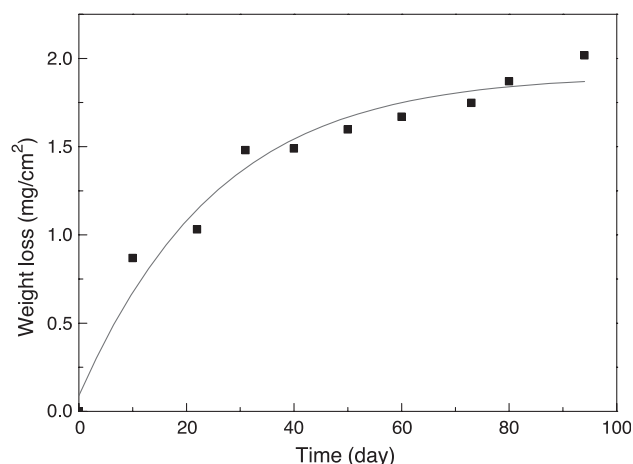


Fig. 4. Weight loss of reinforcing steels in saturated  $\text{Ca(OH)}_2$  with 3.5 wt.% NaCl solution.

steel. The chloride acts as catalysts to corrosion when there is sufficient concentration at the steel surface to break down the passive layer. They are not consumed in the process but help break down the passive layer in the steel and allow the corrosion process to be proceeded quickly [1–3].

Corrosion rate was determined by the Tafel extrapolation method. The corrosion current density can be measured and can yield a corrosion rate based on Faraday's law [9].

$$\text{Corrosion rate (mpy)} = \frac{0.13 i_{\text{corr}} (\mu\text{A}/\text{cm}^2) \times \text{EW}}{\text{Density (g}/\text{cm}^3)}$$

where 0.13 is the metric and time conversion factor and EW is the equivalent weight in grams. Table 1 shows the result of corrosion potential and corrosion rate measured by the Tafel extrapolation method in different solutions. The cor-

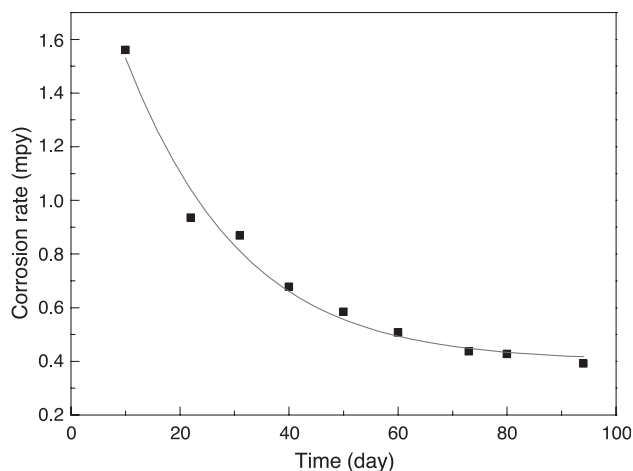


Fig. 5. Corrosion rate of reinforcing steels in saturated  $\text{Ca(OH)}_2$  with 3.5 wt.% NaCl solution.

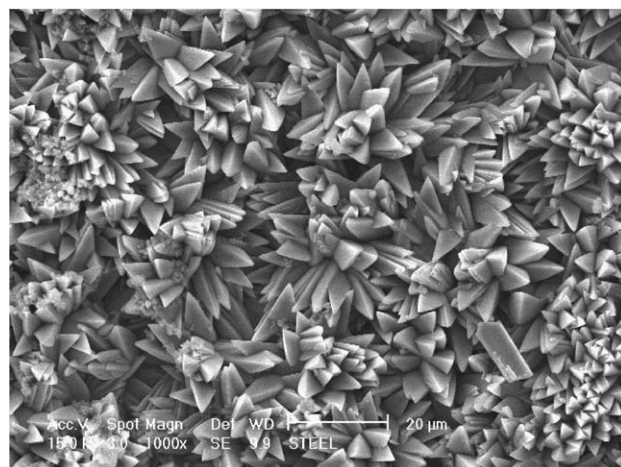


Fig. 6. Surface morphology of the reinforcing steel after the immersion test.

rosion rate of all samples increased with existing chloride ions. However, the anodic behavior above the Tafel region is different between stainless steel and copper. The passive film of stainless steel is broken in that region, while the  $\text{CuCl}$  film of copper starts to build up on the surface. In the case of copper, the magnitudes of the peak current and the current minimum decrease as the  $\text{Cl}^-$  concentration increases [10,11]. Comparison of the polarization results with and without chlorides indicated the possibility of detecting an ingress point in time of chlorides by measuring the galvanic current between the two metals.

### 3.2. Immersion test

Fig. 4 is a plot of the weight loss ( $\text{mg}/\text{cm}^2$ ) of steel (after oxide removal). The weight losses increased rapidly to  $1.5 \text{ mg}/\text{cm}^2$ . With a further increase in the immersion time, a little change in the weight losses was detected. Corrosion rate of the reinforcing steel was determined by using the

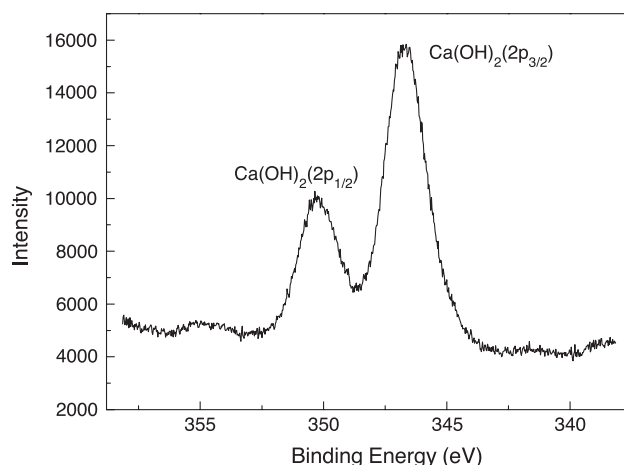


Fig. 7. XPS spectrum of the reinforcing steel after the immersion test.

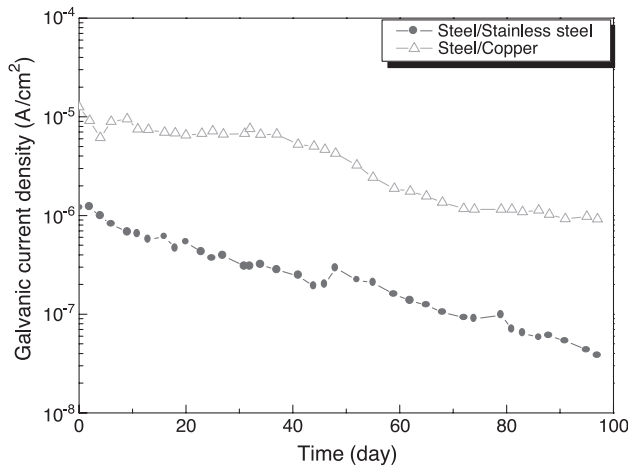


Fig. 8. Galvanic current density versus time.

weight loss method (Fig. 5). The average corrosion rate can be calculated by the following equation [12]:

Corrosion rate(mpy)

$$= \frac{3.45 \times 10^6 \times \text{Weight loss(g)}}{\text{Area(cm}^2\text{)} \times \text{Density(g/cm}^3\text{)} \times \text{Time(h)}}$$

Initially, corrosion rates decreased with time. Then, corrosion rates maintain a steady state with time. This behavior was closely related to the presence of  $\text{Ca(OH)}_2$  at the steel surface as shown in Figs. 6 and 7. These figures show surface morphology and XPS spectrum of the reinforcing steel after the immersion test, respectively.  $\text{Ca(OH)}_2$  crystals can restrain a pH drop at the steel surface. The crystals will thus provide protection against steel corrosion [2].

### 3.3. Galvanic corrosion test

Fig. 8 shows the galvanic current density versus time. The galvanic current density decreased with time. This observa-

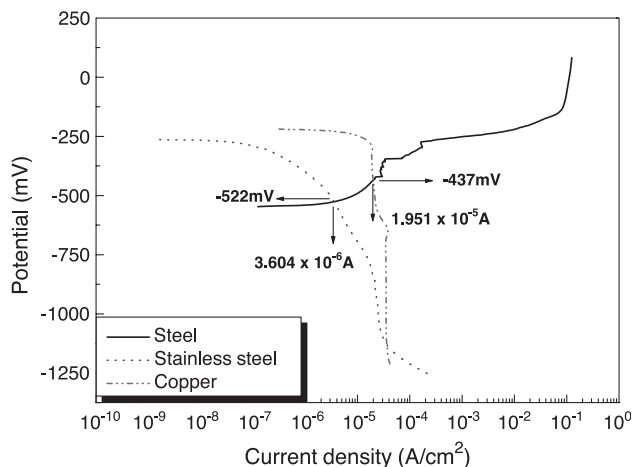
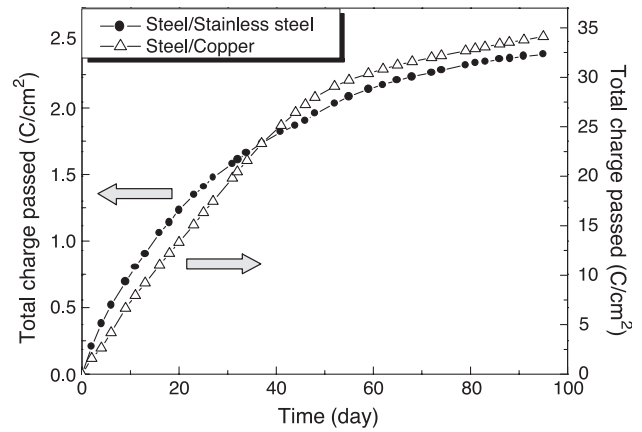


Fig. 9. Anodic polarization curve of reinforcing steel and cathodic polarization curves of stainless steel and copper.

Fig. 10. Output of sensor systems in saturated  $\text{Ca(OH)}_2$  with 3.5 wt.% NaCl solution.

tion would be explained on the basis that  $\text{Ca(OH)}_2$  crystal of specimens restrained a pH drop and reduced the surface area. Generally, if the area of metal is decreased, the curves for both reactions associated with metal (anodic dissolution and

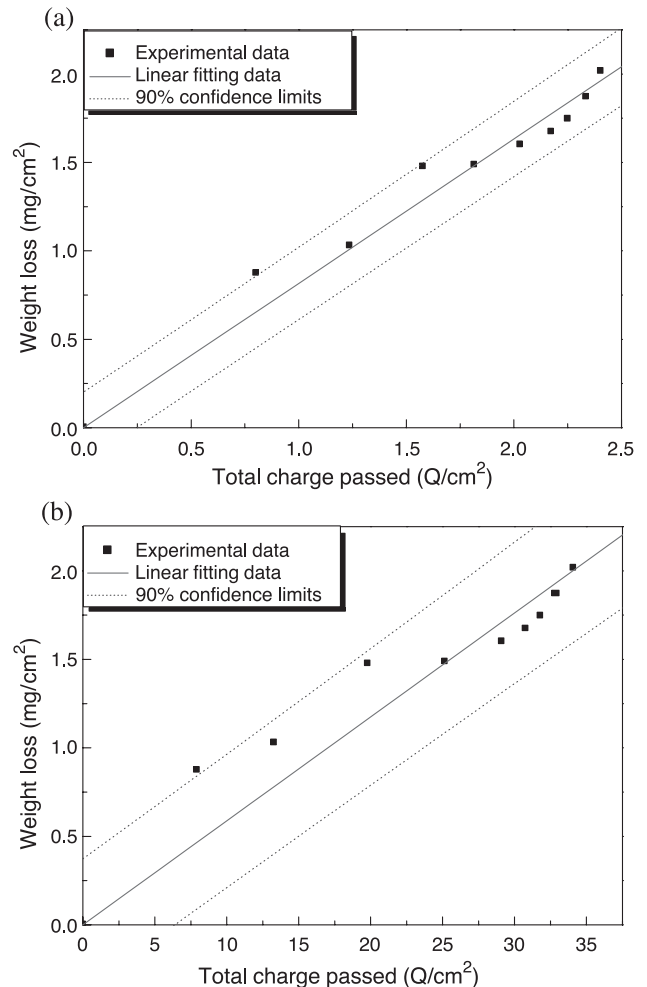


Fig. 11. Weight loss of reinforcing steel and output of sensor system: (a) steel/stainless steel sensor system, (b) steel/copper sensor system.



cathodic reduction on metal) move to the left or to lower values of current proportional to the decrease in area [13]. Also, Fig. 8 indicated that the galvanic current density of steel/copper was higher than that of steel/stainless steel. When steel is coupled to cathode materials in that the galvanic current density is high means that the steel corrodes at a high rate. This result was consistent with predicting galvanic-coupling effects in Fig. 9. According to the polarization curves, the galvanic current in steel/stainless steel is lower than that in steel/copper. Thus, the lifetime of steel/copper sensor is shorter than that of steel/stainless steel sensor. However, it can be assumed that the steel/copper sensor is more suitable for high resistance environment.

Electrochemical reactions either produce or consume electrons. Thus, the rate of electron flow to or from a reacting interface is a measure of reaction rate. Electron flow is conveniently measured as current ( $I$ ) in amperes, where 1 A is equal to  $1\text{ C}$  of charge ( $6.2 \times 10^{18}$  electrons) per second. The galvanic current and time were integrated to the coulomb value based on Faraday's law [14].

$$Q = I \times t = \frac{nFw}{a}$$

where  $F$  is Faraday's constant (96,500 C/equivalent),  $n$  is the number of equivalents exchanged,  $w$  is the weight loss,  $a$  is the atomic weight and  $Q$  is the total coulombs. Fig. 10 presents the correlation between time and total charge using Faraday's law. The rate of increase in the coulomb values decreased as time increased, which means the flow of current between two metals decreased.

Fig. 11 shows the correlation between the coulomb values of the sensor system and the weight loss ( $\text{mg}/\text{cm}^2$ ) of the reinforcing steel. A good correlation was observed in the two systems. The output of steel/stainless steel sensor system showed a better linear correlation than that of steel/copper. Thus, the steel/stainless steel sensor system is better reliable. The current flows in the galvanic sensor are representative of what is happening in the steel and how much corrosion on the reinforcing steel of a real structure is occurring. However, the galvanic current cannot be detected when the resistance of the concrete is too high to support the galvanic cell. In case the resistance of the concrete is high, the steel/copper sensor can be effective due to the high galvanic current.

#### 4. Conclusions

The investigation of a galvanic sensor system for detecting the corrosion damage shows the following results:

1. The galvanic sensor system can provide a useful nondestructive method of determining actual corrosion

rate. This was conformed by electrochemical experiments in the laboratory.

2. An ingress point in time of chlorides can be detected by measuring the galvanic current between the two metals.
3. The output of steel/stainless steel sensor system showed a better linear correlation than that of steel/copper. Nevertheless, the steel/copper sensor is more suitable for high-resistance environment due to the high current output.

#### Acknowledgements

The authors wish to acknowledge the financial support of the Korea Science and Engineering Foundation (KOSEF) for the National Research Laboratory (NRL) project M1-0203-00-0068.

#### References

- [1] J.P. Broomfield, Corrosion of Steel in Concrete, E & FN Spon, London, 1997, p. 22.
- [2] T. Yonezawa, V. Ashworth, R.P.M. Procter, Pore solution composition and chloride effects on the corrosion of steel in concrete, Corrosion 44 (1988) 489–499.
- [3] M.F. Montemor, A.M.P. Simoes, M.M. Salta, Effect of fly ash on concrete reinforcement corrosion studied by EIS, Cem. Concr. Compos. 22 (2000) 175–185.
- [4] B. Borgard, C. Warren, S. Somayaji, R. Heidersbach, Mechanisms of Corrosion of Steel in Concrete, ASTM STP 1065, Philadelphia, 1990, p. 174.
- [5] B. Elsener, Macrocell corrosion of steel in concrete—implications for corrosion monitoring, Cem. Concr. Compos. 24 (2002) 65–72.
- [6] C. Arya, P.R.W. Vassie, Influence of cathode-to-anode area ratio separation distance on galvanic corrosion currents of steel in concrete containing chlorides, Cem. Concr. Res. 25 (1995) 989–998.
- [7] J. Gulikers, Development of a galvanic monitoring probe to improve service life prediction of reinforced concrete structures with respect to reinforcement corrosion, Constr. Build. Mater. 11 (1997) 143–148.
- [8] M. Raupach, P.P. Schiessl, Monitoring system for the penetration of chlorides, carbonation and the corrosion risk for the reinforcement, Constr. Build. Mater. 11 (1997) 207–214.
- [9] S.W. Dean, Handbook on Corrosion Testing and Evaluation, Wiley, New York, 1971, p. 171.
- [10] H.P. Lee, K. Nobe, Kinetics and mechanisms of Cu electrodisolution in chloride media, J. Electrochem. Soc. 133 (1986) 2035–2043.
- [11] A.V. Benedetti, P.T.A. Sumodjo, K. Nobe, P.L. Cabot, W.G. Proud, Electrochemical studies of copper, copper–aluminum and copper–aluminum–silver alloys, Electrochim. Acta 40 (1995) 2657–2668.
- [12] ASTM Standard G31, Standard practice for laboratory immersion corrosion testing of metals, 1994 Book of ASTM Standards, vol. 03.02, ASTM, West Conshohocken, 1994, p. 102.
- [13] R.A. Buchanan, Fundamentals of Electrochemical Corrosion, ASM International, Ohio, 2000, p. 164.
- [14] D.A. Jones, Principles and Prevention of Corrosion, Prentice-Hall, London, 1996, pp. 75–86.